

## Potentials and glueballs at large beta in SU(2) pure gauge theory

This article has been downloaded from IOPscience. Please scroll down to see the full text article.

1992 J. Phys. G: Nucl. Part. Phys. 18 1725

(<http://iopscience.iop.org/0954-3899/18/11/005>)

[The Table of Contents](#) and [more related content](#) is available

Download details:

IP Address: 143.233.227.239

The article was downloaded on 13/11/2009 at 12:32

Please note that [terms and conditions apply](#).

# Potentials and glueballs at large beta in $SU(2)$ pure gauge theory

C Michael and S J Perantonis

DAMTP, Liverpool University, Liverpool L69 3BX, UK

Received 30 July 1991

**Abstract.** Interquark potentials and the glueball mass spectrum are evaluated from  $32^4$  lattices for pure  $SU(2)$  gauge fields at  $\beta = 2.5, 2.7$  and  $2.9$ . We discuss scaling and asymptotic scaling. Results for excited states are presented, including a reliable mass value for a  $J^P$  exotic glueball.

## 1. Introduction

The relevance of lattice gauge theory to continuum QCD depends on the assumption that the limit of small lattice spacing is well behaved. For a physical quantity, such as a mass, the combination  $aM$  is actually measured and when  $a$  decreases with increasing  $\beta$ , as prescribed by the two-loop perturbative beta function, this is called asymptotic scaling. For  $\beta > 2.4$  for  $SU(2)$  and  $\beta > 6.0$  for  $SU(3)$ , lattice observables show [1] a decrease of  $a$  with  $\beta$  which seems to be the same for several observables but which is faster than asymptotic scaling. If ratios of physical quantities are indeed constant for present  $\beta$  values and beyond then one has valid predictions for the continuum limit. It is still of interest, however, to increase  $\beta$  further until the region of asymptotic scaling is reached in order to be able to relate lattice observables to the perturbative coupling given in terms of  $\Lambda_{\text{MSB}}$ . A recent Monte Carlo renormalization graph (MCRG) analysis on  $32^4$  lattices [2] for  $SU(2)$  obtains the result that asymptotic scaling is not restored even at  $\beta = 2.9$ .

In order to explore this approach to the continuum limit in more detail, we complement the MCRG analysis by measuring directly several physical quantities on large lattices at large  $\beta$ . The quantities that we are able to measure accurately are the potential between static quarks, the energy of the flux loop encircling the periodic boundary (the torelon) and the glueball spectrum. This will allow us to study with increasing  $\beta$  the ratio of different physical quantities as well as the lattice spacing  $a$  itself.

Since we wish to study the continuum limit in a large volume to calibrate lattice gauge theory as a physical tool, we need to perform simulations at large  $\beta$  with a large spatial lattice volume. Such simulations will be affected by critical slowing down and to have a realistic exploration it is preferable to use  $SU(2)$  colour fields, since the computing resource is much less than for  $SU(3)$  colour. Thus we follow [2] and use  $32^4$  lattices at  $\beta = 2.5, 2.7$  and  $2.9$ . Moreover we use a number of their configurations as starting configurations. Our update code is our own although we

also choose to use the same update algorithm: namely several over-relaxation sweeps [3] per heat-bath sweep. They measure autocorrelation times (defined as correlation = 0.25) for spatially extended operators of 40 sweeps at  $\beta = 2.7$  and 300 sweeps at  $\beta = 2.9$ . We measure every four sweeps and collect data into blocks of 100 sweeps for analysis. As expected, these blocks are consistent with being independent for  $\beta < 2.9$ . For  $\beta = 2.9$ , we will have significant correlation between our blocks of 100 sweeps although making use of several independent starting configurations (widely separated from [2]) enables us to obtain sensible estimates of averages. As we shall discuss later, there are also systematic errors arising at  $\beta = 2.9$  from the limited time extent of our lattice so our results will only be indicative at that  $\beta$  value.

In order to have reliable measurements of physical (and thus extended) objects, it is important to use extended and smooth operators. We find that methods used previously at smaller  $\beta$  values can be extended easily to the  $\beta$  values used in this work. The glueball and torelon observables are obtained from correlations measured using fuzzing (Teper blocking [3]) and a variational path basis in the manner of [4]. For the potential determinations, we use  $R \times T$  Wilson loops with a careful choice for the spatial strings of length  $R$  at each end. Thus we first fuzz [3] the spatial links of the lattice once to a  $16^3 \times 32$  effective lattice and then use smearing [5] and a variational path basis in the manner of [6, 7]. We also use multihit links [8] in the  $t$  direction. The potentials at separations which are a multiple of two lattice spacings are then determined using Wilson loop ratios at adjacent  $t$  values as in [7]. We now report our results for the potentials and glueball mass spectrum.

## 2. Potentials

The dimensionless quantity measured is  $aV(R)$  versus  $R/a$ . We have results for the ground-state potentials within the irreducible representations  $A_{1g}$ ,  $E_u$  and  $A_{1u}$  of the symmetry group  $D_{4h}$  of the gluonic configuration between the static sources.

Using the combined fuzzing and blocking technique we are able to obtain high overlaps (comparable to the ones obtained in our earlier work at smaller  $\beta$  values [7]) between the operators used and the ground state in each representation, without excessive computational effort. Thus with a blocking coefficient  $C$  (defined as in [7]) equal to 2.5 and with blocking levels in the range 8–40 we obtained optimal overlaps for the  $\beta$  values studied. Details of the Monte Carlo simulations and measurements for the potentials are given in table 1. Results for the potentials are shown in tables 2–4. The results are obtained by requiring that the potential estimates from two adjacent  $t$  ratios are consistent. In most cases these are 4/3 and 5/4  $t$  ratios. Then the error quoted is the statistical error associated with the

**Table 1.** Details of our Monte Carlo simulations and measurements for the potentials.

$\beta$	Number of updates	Lattices measured	Blocking level	Range of $R/a$	Range of $t$
2.5	1500	375	8	2–22	0–5
2.7	2000	500	25	4–22	0–5
2.9	2700	675	40	4–22	0–5

**Table 2.** Values for the ground-state and excited potentials (in inverse lattice spacing units) as a function of the source separation at  $\beta = 2.5$ .

$R/a$	$A_{1g}$	$E_u$	$A_{1u}$
2	0.4836 (3)	1.119 (7)	1.146 (14)
4	0.6229 (5)	1.089 (4)	1.165 (6)
6	0.7154 (12)	1.088 (4)	1.200 (9)
8	0.7970 (17)	1.110 (4)	1.254 (12)
10	0.8745 (25)	1.148 (5)	1.315 (13)
12	0.9514 (46)	1.194 (5)	1.393 (17)
14	1.0300 (41)	1.243 (7)	1.438 (19, -22)
16	1.1063 (54)	1.303 (9)	1.515 (34)
18	1.1784 (139)	1.352 (10, -15)	1.592 (37)
20	1.2583 (108)	1.412 (12, -18)	1.704 (19)
22	1.3396 (204)	1.493 (24)	1.799 (34)

potential at the larger  $t$  value of two adjacent  $t$  values that agree. In the few cases that agreement is not reached even for the  $5/4$   $t$  ratio, the difference between the estimates from  $4/3$  and  $5/4$   $t$  ratios is quoted as a systematic error in our estimate.

Our results agree well with previous results at  $\beta = 2.5$  from a  $20^4$  lattice [7]. The lattice potential between static sources has a self-energy component which diverges as  $a \rightarrow 0$ , so only potential differences are physical. The most straightforward way to compare potentials at different  $\beta$  values is to make fits to the  $R$  dependence. The statistical errors on the potentials at different  $R$  values are somewhat correlated but the full correlation matrix for 12  $R$  values is rather unstable when inverted if the number of data sub-samples is not much bigger than 12. Thus to weight the different  $R$  values in the fit, we use the diagonal errors only. We find that fits of the form

$$aV(R) = c - Ea/R + Ka^2R/a$$

at the three  $\beta$  values are statistically acceptable and determine the value of the string tension  $K$  in lattice units. Note that a lattice version of the Coulomb term is used in the fits. Our results from these fits are shown in table 5. The errors quoted for the parameters  $c$ ,  $E$  and  $K$  in table 5 are from the fit using the diagonal errors on the potentials only and so should be overestimates.

**Table 3.** Values for the ground-state and excited potentials (in inverse lattice spacing units) as a function of the source separation at  $\beta = 2.7$ .

$R/a$	$A_{1g}$	$E_u$	$A_{1u}$
4	0.4771 (3)	0.809 (4)	0.817 (6)
6	0.5182 (6)	0.801 (4)	0.817 (6)
8	0.5494 (10)	0.798 (4)	0.825 (6)
10	0.5767 (13)	0.800 (4)	0.835 (7)
12	0.6023 (18)	0.806 (4)	0.849 (7)
14	0.6269 (22)	0.815 (5)	0.864 (8)
16	0.6512 (27)	0.825 (5)	0.881 (9)
18	0.6754 (32)	0.837 (5)	0.898 (10)
20	0.6997 (37)	0.849 (6)	0.914 (10)
22	0.7238 (43)	0.863 (7)	0.932 (11)
24	0.7478 (47)	0.880 (8)	0.951 (12)

**Table 4.** Values for the ground-state and excited potentials (in inverse lattice spacing units) as a function of the source separation at  $\beta = 2.9$ .

$R/a$	$A_{1g}$	$E_u$	$A_{1u}$
4	0.4016 (2)	0.653 (4, -5)	0.662 (6)
6	0.4265 (3)	0.645 (4, -5)	0.658 (6)
8	0.4422 (5)	0.641 (4)	0.659 (7)
10	0.4541 (7)	0.640 (4)	0.661 (7)
12	0.4644 (9)	0.639 (4)	0.665 (7)
14	0.4735 (11)	0.640 (4)	0.669 (8)
16	0.482 (2)	0.641 (4)	0.673 (8)
18	0.490 (2)	0.643 (4)	0.678 (8)
20	0.498 (2)	0.646 (4)	0.683 (9)
22	0.506 (3)	0.650 (4, -5)	0.688 (9)
24	0.514 (3, -4)	0.654 (5)	0.694 (9)

These fits show a significant decrease of the coefficient  $E$  with increasing  $\beta$  which can be understood as a decrease of the Coulomb strength with decreasing  $g^2$ . This is expected since the continuum renormalization-group improved expression behaves like  $1/R \ln(\Lambda R)^{-2}$  and our analysis probes smaller  $R$  at larger  $\beta$ . Thus we find that a common fit for the  $A_{1g}$  potential with a common value of  $E$  for all three  $\beta$  values is not statistically acceptable.

In figure 1 we show the values for the  $A_{1g}$ ,  $E_u$  and  $A_{1u}$  potentials in a common graph in the  $R$  region where we have results for at least two  $\beta$  values. The  $A_{1g}$  potentials for different  $\beta$  values are assumed to coincide at  $R = \infty$ .

From our results for  $Ka^2$  one obtains  $a(2.5):a(2.7):a(2.9)$  of 1.80(2) and 1.81(3) respectively. The two loop perturbative ratio at  $\beta = 2.7$  for a change of 0.2 in  $\beta$  is 1.66. Thus one might conclude that perturbative scaling is not restored even at  $\beta = 2.9$ . This result is in agreement with results from a recent MCRG analysis [2]. However, the results at  $\beta = 2.9$  should be treated with caution, because there is a possibility that the finite-size effects are very important. The ratio of excited gluonic potentials to the ground-state potential is different (see figure 1), rotational invariance is not restored (see glueball section), etc. Thus a determination of scaling up to  $\beta = 2.9$  by a direct comparison with the large-volume physical quantities measured at  $\beta = 2.5$  and 2.7 is not justified, since at  $\beta = 2.9$  there are significant finite-size effects. On the other hand, we find that the excited potentials at  $\beta = 2.5$  and  $\beta = 2.7$  scale according to the same  $a$  ratio as for the  $A_{1g}$  potential scaling within the errors (to the error shown in figure 1 originating from the statistical error in the determination of the Wilson loop ratios at  $\beta = 2.7$ , we must superimpose errors in the determination of the lattice spacing and the self energy constant  $c$ . When these are taken into account, there is clear evidence of scaling of the excited potentials within the total error in their determination). Consistent results between  $\beta = 2.5$  and

**Table 5.** Details of the linear plus lattice Coulomb fits to the results for the  $A_{1g}$  potentials.

$\beta$	2.5	2.7	2.9
$Ka^2$	0.0363 (3)	0.0112 (2)	0.00342 (14)
$c$	0.527 (2)	0.478 (3)	0.432 (2)
$E$	0.234 (3)	0.214 (9)	0.208 (5)

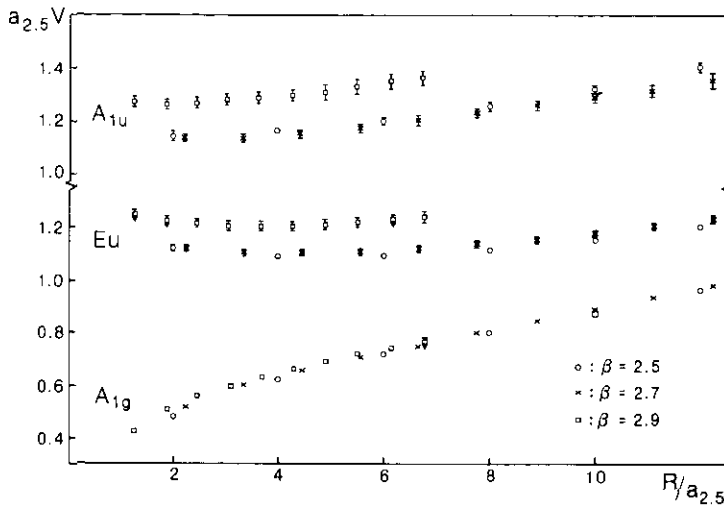


**Figure 1.** Potentials between static colour sources at separation  $R$ . The curves labelled  $A_{1g}$  are the usual potentials whereas those labelled  $E_u$  and  $A_{1u}$  refer to the low-lying gluonic excitations of the potential (for which the gluon field has non-zero angular momentum component about the separation axis). Data at three  $\beta$  values have been combined using  $a(2.5):a(2.7):a(2.9)$  of 1.80 and 1.81, respectively. The errors shown originate from the statistical errors in the determination of Wilson loop ratios at adjacent  $t$  values.

$\beta = 2.7$  are also obtained for the glueballs. We can thus safely conclude that we have a reliable determination of the ratio of the physical values of the lattice spacing from  $\beta = 2.5$  to  $\beta = 2.7$ . Our results for the comparison of  $\beta = 2.5$  and 2.7 correspond to a  $\beta$  function which is 80% of the perturbative value—in agreement with the MCRG analysis of [2].

As in previous work [6, 7], we can compare the excited  $E_u$  and  $A_{1u}$  potentials with string model predictions. Potential results for  $\beta = 2.5$  are shown in figure 2 where the predictions of models for the non-relativistic bosonic string and the

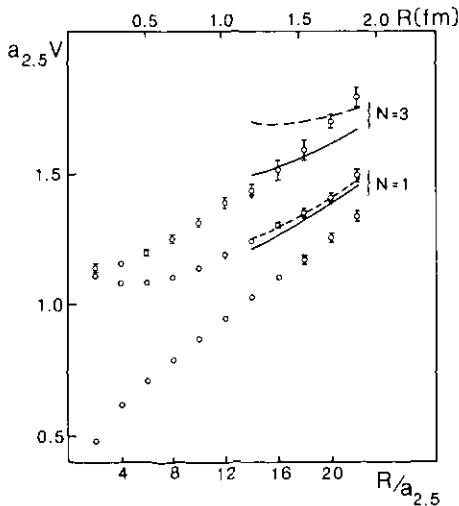


**Figure 2.** The  $A_{1g}$ ,  $E_u$  and  $A_{1u}$  potentials at  $\beta = 2.5$  for source separations up to 1.88 fm (the physical length scale is set by the value of the string tension  $\sqrt{K} = 0.44$  GeV). Predictions of the relativistic (solid line) and the non-relativistic (dashed line) bosonic string models for the excited potentials are also shown.  $N = 1$  and  $N = 3$  correspond to the predictions for the  $E_u$  and  $A_{1u}$  potential, respectively.

relativistic bosonic string with fixed ends [9, 10] are also depicted. String models predict an energy difference between the excited potentials and the  $A_{1g}$  potential with a leading behaviour of  $N\pi/R$  at large  $R$ , where  $N = 1$  for the  $E_u$  and  $N = 3$  for the  $A_{1u}$ . As shown in figure 2, the predictions of different string models for the  $E_u$  potential are similar for  $R \geq 1.2$  fm (with the physical scale set by the usual value for the string tension of  $\sqrt{K/a} = 0.44$  GeV) and string models are seen to provide a very good guide for the pure gauge theory  $E_u$  potential. However, the predictions of different string models for the  $A_{1u}$  potential differ substantially even at  $R = 1.88$  fm (the largest source separation we have studied). The  $A_{1u}$  potential, as determined from pure  $SU(2)$  lattice gauge theory, is in the general region expected by string models for  $R \geq 1.4$  fm. Note that for the excited potentials at the largest  $R$  values, the statistical errors are largest and thus the systematic error associated with the extrapolation to large  $t$  values is inherently larger. This may explain the apparent steep rise at the largest  $R$  values for our determination of the  $A_{1u}$  potential at  $\beta = 2.5$ .

These gluonic excitations are relevant for hybrid meson spectroscopy. For applications to experiment, it is preferable to use  $SU(3)$  colour and recent results exist [6] which give predictions for spin-exotic hybrid mesons near the  $B\bar{B}$  threshold. These gluonic excitations are quite close in energy to the  $A_{1g}$  ground state at large  $R$  and there are many such excited levels. This has implications for the extraction of the ground-state interquark potential using Wilson line methods [11]. Because of completeness, all excited levels contribute in this case which may explain the discrepancy between string tension results obtained using Wilson line correlations and those using the conventional method (as used here).

### 3. Glueballs

The glueball results on  $32^4$  lattices are presented in tables 6–8. The extrapolated mass and error are shown in bold. These results are obtained by requiring that the

**Table 6.** Glueball and torelon effective masses in lattice units at  $\beta = 2.5$ . The extrapolated values are shown in bold. The non-zero momentum results have  $p^2 < 13(\pi/16)^2$ . Results are from measurements of 475 lattices (375 for torelons).

Rep	$J^P$	1/0	2/1	3/2	4/3
$A_1^+$	$0^+$	0.74 (3)	<b>0.70 (4)</b>	0.62 (6)	0.56 (13)
		$p \neq 0$	0.74 (1)	<b>0.69 (3)</b>	0.69 (6)
$E^+$	$2^+$	1.13 (1)	<b>0.99 (4)</b>	1.02 (13)	0.79 (30)
$T_2^+$		$p \neq 0$ :	1.11 (2)	<b>1.08 (6)</b>	1.15 (20)
$A_1^-$	$0^-$	1.22 (1)	<b>1.11 (3)</b>	1.28 (21)	1.08 (59)
$E^-$	$2^-$	1.51 (3)	1.37 (14)		
$T_2^-$		1.59 (3)	1.42 (11)	1.36 (45)	
$A_2^+$	$3^+$	1.64 (2)	1.24 (9)	0.74 (18)	
$T_1^+$	$1^+$	<b>1.88 (4)</b>	1.95 (43)		
$A_2^-$	$3^-$	2.07 (3)	1.70 (20)	0.89 (42)	
$T_1^-$	$1^-$	2.76 (12)			
$A(100)$		2.30 (5)			
$A(110)$		1.32 (2)	1.22 (5)	<b>1.08 (15)</b>	0.88 (53)
$B(110)$		2.57 (9)	1.59 (45)		
$A(111)$		2.39 (5)	1.74 (39)		
		5.07 (128)			

**Table 7.** Glueball and torelon effective masses in lattice units at  $\beta=2.7$ . The extrapolated values are shown in bold. The non-zero momentum results have  $p^2 < 5(\pi/16)^2$ . Results are from measurements of 725 lattices.

Rep	$J^P$	1/0	2/1	3/2	4/3	
$A_1^+$	$0^+$	0.44 (2)	0.40 (3)	<b>0.39 (3)</b>	0.41 (4)	
$E^+$	$2^+$	$p \neq 0$ :	0.49 (3)	0.43 (4)	<b>0.40 (5)</b>	
		$p \neq 0$ :	0.65 (1)	0.57 (2)	<b>0.55 (3)</b>	0.53 (4)
$T_2^+$	$2^+$	$p \neq 0$ :	0.71 (3)	0.60 (4)	<b>0.56 (7)</b>	
$A_1^-$		$0^-$	0.69 (1)	0.62 (2)	0.56 (2)	<b>0.53 (4)</b>
$E^-$	$2^-$	$p \neq 0$ :	0.83 (2)	0.67 (3)	<b>0.63 (6)</b>	0.68 (12)
$T_2^-$		0.91 (2)	0.79 (3)	<b>0.73 (5)</b>		
$A_2^+$	$3^+$	0.90 (1)	0.77 (2)	<b>0.72 (4)</b>		
$T_1^+$	$1^+$	1.08 (2)	<b>0.90 (5)</b>	0.94 (13)		
$A_2^-$	$3^-$	1.17 (1)	<b>1.02 (3)</b>	1.07 (8)		
$T_1^-$	$1^-$	1.50 (3)	1.32 (11)			
$A(100)$		1.27 (1)	1.11 (4)	<b>1.10 (10)</b>		
$A(110)$		0.34 (1)	0.30 (1)	<b>0.29 (1)</b>	0.29 (2)	
$B(110)$		0.65 (2)	0.55 (2)	<b>0.54 (3)</b>	0.57 (5)	
$A(111)$		0.49 (2)	0.41 (2)	<b>0.39 (3)</b>	0.37 (4)	
		1.01 (4)	0.82 (6)	<b>0.82 (9)</b>	0.90 (25)	

effective mass at two adjacent  $t$  ratios is consistent. In most cases these are 2/1 and 3/2  $t$  ratios. Then the error quoted is the statistical error associated with the effective mass at the larger  $t$  value of two adjacent  $t$  values that agree. From these effective mass values one sees that those determined from the  $t$  ratio 0/1 values are only slightly higher than those from large  $t$  ratios, which implies that the overlap of the fuzzy path combination used is excellent: it has a big projection on the ground-state glueball with very little excited-state contribution. This is essential to explore larger  $\beta$  with small statistical errors and our results confirm the continued success of Teper fuzzing at large  $\beta$ .

The results at  $\beta = 2.5$  agree with previous  $20^4$  results [4] which is to be expected

**Table 8.** Glueball and torelon effective masses in lattice units at  $\beta=2.9$ . The extrapolated values are shown in bold. The non-zero momentum results have  $p^2 < 5(\pi/16)^2$ . Results are from measurements of 625 lattices.

Rep	$J^P$	1/0	2/1	3/2	4/3	
$A_1^+$	$0^+$	0.30 (2)	0.25 (2)	<b>0.25 (2)</b>	0.25 (3)	
$E^+$	$2^+$	$p \neq 0$ :	0.34 (4)	0.29 (6)	<b>0.27 (7)</b>	
		$p \neq 0$ :	0.47 (2)	0.39 (2)	<b>0.39 (3)</b>	0.36 (4)
$T_2^+$	$2^+$	$p \neq 0$ :	0.47 (2)	<b>0.45 (3)</b>	0.41 (5)	
$A_1^-$		$0^-$	0.53 (1)	0.48 (1)	0.45 (2)	0.42 (2)
$E^-$	$2^-$	$p \neq 0$ :	0.67 (2)	0.61 (3)	0.49 (4)	<b>0.48 (6)</b>
$T_2^-$		0.72 (1)	0.62 (3)	<b>0.56 (4)</b>	0.54 (5)	
$A_2^+$	$3^+$	0.72 (1)	0.62 (2)	<b>0.62 (3)</b>	0.57 (5)	
$T_1^+$	$1^+$	0.83 (2)	0.78 (3)	<b>0.76 (7)</b>	0.69 (13)	
$A_2^-$	$3^-$	0.90 (1)	0.81 (2)	<b>0.76 (6)</b>	0.84 (10)	
$T_1^-$	$1^-$	1.32 (3)	1.13 (9)	0.79 (16)		
$A(100)$		1.02 (1)	0.88 (2)	<b>0.88 (6)</b>	0.88 (15)	
$A(110)$		0.95 (7)	0.086 (6)	<b>0.082 (6)</b>	0.081 (6)	
$B(110)$		0.18 (1)	0.15 (1)	<b>0.14 (1)</b>	0.14 (1)	
$A(111)$		0.14 (1)	0.12 (1)	<b>0.12 (1)</b>	0.11 (1)	
		0.30 (3)	0.27 (3)	<b>0.25 (3)</b>	0.25 (4)	



since the respective  $Z$  values ( $M(0^+)L$ ) are 14.4 and 22.4 which both lie in the large-volume regime of  $Z > 9$ .

For the results at  $\beta = 2.7$ , one sees that rotational invariance is restored in the two determinations of the  $J = 2$  states. This is again expected since the  $Z$  value of 12.4 is in the large-volume regime. We also obtain consistency between momentum zero and non-zero observables: restoration of Lorentz boost invariance. A level ordering of these lightest glueball states versus  $J^P$  is also clear. The dimension-4 operators ( $GG$ ) couple to  $0^+$ ,  $2^+$ ,  $0^-$  and  $2^-$ ; then dimension-5 operators like  $GDG$  couple to  $1^+$  and  $3^+$ ; while the  $J^P$ -exotic states  $1^-$  and  $3^-$  need dimension-6 operators like  $GGG$ .

This is the first reliable determination of the mass spectrum of a  $J^P$ -exotic glueball state. Even so, the mass value is relatively large with  $M(1^-)/M(0^+) = 2.8(5)$ . Note that previous work shows that the glueball mass ratios for positive charge conjugation states are identical within errors for  $SU(2)$  and  $SU(3)$  pure gauge theory [1], so this exotic- $J^P$  result may give a useful indication of the mass value of the exotic  $1^-$  glueball for  $SU(3)$  pure gauge theory.

Our glueball spectrum results at  $\beta = 2.9$  come from the same analysis as at the lower  $\beta$  values. However, the  $A(100)$  torelon energy is now very low which implies that one cannot neglect torelon propagation 'round the back'. Thus  $\exp(-32E) = 0.072$  for the  $A(100)$  torelon and, moreover, the torelon can have three independent orientations. This implies that our extraction of transfer matrix eigenstates can be in error. A detailed discussion of the mechanism is given in the appendix. The results of table 9, however, show no sign of any such torelon contamination effect. We conclude that the method used gives sensible estimates of the mass spectrum but with an unknown systematic error. The way to improve on this situation is to use  $32^3 \times T$  lattices with  $T \gg 32$ .

Taking our results at  $\beta = 2.9$  at face value, they show that finite-volume effects may be important. This is expected because the value of  $Z$  (defined as  $M(0^+)L$ ) is about 8 which is in the region where finite-size effects become important at smaller  $\beta$ . Also we see significant differences between the  $E^+$  and  $T_2^+$  masses so that rotational invariance is not restored. Thus we should not compare the 2.9 results directly with lower  $\beta$  large-volume results.

A study of scaling using large-volume physical results can thus only be made up to  $\beta = 2.7$ . Between  $\beta = 2.5$  and 2.7, the ratio  $a(2.5)/a(2.7)$  is found to be consistent with that obtained from the string tension analysis above but the errors are larger in the glueball analysis (ratios are 1.79(19) for  $0^+$  and 1.91(20) for  $2^+$ ).

Another observable is the torelon: the energy of a unit of colour flux encircling the periodic spatial boundary. We actually measure the energies of torelons encircling one (100), two (110) and three (111) orthogonal boundaries and we classify the torelons encircling two boundaries as even  $A(110)$  or odd  $B(110)$  under rotation by  $90^\circ$  about the third direction. The energy per unit length of the  $A(100)$  torelon gives an effective string tension.

At  $\beta = 2.7$ , we obtain  $a^2 K_{\text{eff}} = 0.0091(4)$  which is significantly smaller than the value of 0.0112(2) obtained from the analysis of the potential. It is known empirically [1] from lower  $\beta$  results that  $K_{\text{eff}}$  is reduced at finite  $L$ . A theoretical analysis of string fluctuation on a  $L \times \infty^2$  spatial lattice yields [12] the correction  $K = K_{\text{eff}} + \pi/3L^2$ . This correction would give  $a^2 K = 0.0101(4)$  from the above torelon energy and presumably an even larger correction [1] applies to a  $L^3$  spatial lattice rather than a  $L \times \infty^2$  one. Thus there is no disagreement between the two

methods of determining the string tension, each with their own systematic errors. Combining these results gives  $a^2K = 0.0110(4)$  which yields  $\sqrt{K}/\Lambda_L = 48.6(1.0)$  using the conventional definition of  $\Lambda_L$ . Within errors, the other torelon energy values are also consistent with a string picture: namely energies in the ratio  $1:\sqrt{2}$  for (100) and (110) torelons, respectively.

Indeed at  $\beta = 2.5$ , where the spatial size is much bigger, the torelon energy gives  $a^2K_{\text{eff}} = 0.034(4)$  which is completely consistent with the potential determination. Note that in this case the torelon flux is of length  $32a(2.5)$  which is  $6/\sqrt{K}$  or 2.7 fm with the conventional string tension value (0.44 GeV). This is the largest distance to which linear confinement in pure gauge theory has been tested. This is illustrated in figure 2.

#### 4. Conclusions

We have confirmed that fuzzing of observables is a very efficient method of extracting energy eigenvalues even at as large a  $\beta$  value as 2.9. Static quark potentials, gluonically excited potentials, torelons and glueballs have all been studied with high precision. Scaling between  $\beta = 2.5$  and  $\beta = 2.7$  is seen for all of these observables. We do not find asymptotic scaling in this region—in agreement with MCRG studies [2]. We determine the string tension ( $\sqrt{K}/\Lambda_L = 49(1)$  for  $SU(2)$  pure gauge theory at  $\beta = 2.7$ ) closer to the continuum limit than hitherto. Our glueball spectrum at  $\beta = 2.7$  is very precise and shows a convincing signal for a  $J^P$ -exotic state ( $1^-$ ) for the first time.

Many MCRG results (see 2 for a summary) at large  $\beta$  have been obtained. These analyses have necessarily used small spatial volumes. We now know [13] that for  $M(0^+)L < 5$ , the vacuum is well approximated by Gaussian fluctuations around a spatially homogeneous colour field. This is very different from the large-volume regime ( $M(0^+)L > 9$ ) which has colour excitations on many length scales. These observations imply that to study the large-volume continuum limit in lattice gauge theory, it is essential to perform the simulations at large volume. Thus our present work satisfies this requirement up to  $\beta = 2.7$  for  $SU(2)$ . To study  $\beta = 2.9$ , one would need a  $48^3$  spatial lattice. Indeed it is worthwhile to study  $64^4$  lattices if possible to extend the  $\beta$  range even further. Only in this way will we be able to calibrate the approach to the continuum limit in lattice gauge theory.

#### Appendix

The correlation we measure between closed spatial paths  $P$  at times 0 and  $t$  can be expressed in terms of the complete set of transfer matrix eigenvectors  $|\alpha\rangle$ :

$$\langle P_0 P_t \rangle = \sum_{\alpha\beta} \lambda_\alpha^{T-t} \langle \alpha | P_0 | \beta \rangle \lambda_\beta^t \langle \beta | P_t | \alpha \rangle / \sum_\alpha \lambda_\alpha^T$$

At large  $T$  and relatively small  $t$ , it is usually possible /to restrict  $\alpha$  to the vacuum level (with  $\lambda_0 = 1$ ) only provided that  $\lambda_\alpha^T \ll 1$  for all excited states. To investigate this, consider the eigenvalues which are of two kinds: the zero electric flux sector (vacuum and glueballs) and the non-zero electric flux sector (torelons). In general

when finite-size effects are important the torelon states lie lower in energy than the glueball states and are thus *a priori* more important [14]. In some cases, however, there may be symmetry reasons (the  $Z(2)$  electric flux invariance of the pure gauge lattice theory) why torelon effects are irrelevant. We study this in general here. Consider first glueball observables.

Since the paths  $P$  used to study glueballs are closed and do not encircle the boundary (mod 2), they have matrix elements  $\langle \text{torelon} | P | \text{glueball or vacuum} \rangle$  which are zero. Thus the predominant effect of light torelon states is through matrix elements  $\langle \text{torelon} | P | \text{torelon} \rangle$  with a torelon state running around the whole  $T$  extent, so with eigenvalue  $\lambda^T$  or  $\exp(-ET)$  where  $E$  is its energy. Since the lightest torelon state (the  $A(100)$ ,  $A(010)$  and  $A(001)$  triplet of  $x$ ,  $y$ , and  $z$ -directed electric flux states) transforms as a representation of the discrete symmetry group  $D_{4h}$ , the way to check whether  $\langle \text{torelon} | P | \text{torelon} \rangle$  is zero from symmetry arguments is to subduce the  $O_h$  representation to which  $P$  transforms to  $D_{4h}$  and then use the Clebsch–Gordan series for  $D_{4h}$ . This indicates that  $A(100)$  torelons contribute to the  $E^+$  path correlation (since  $E^+$  subduces to  $A_{1g}$  among other representations). Thus the observed correlation will behave as

$$\langle P_0 P_t \rangle = \langle g | P | g \rangle^2 (\lambda_g^t + \lambda_g^{T-t}) / (1 + 3\lambda_A^T) + 3 \langle A | P | A \rangle^2 \lambda_A^T$$

to order  $\lambda_A^T$  (which is  $\exp(-E_A T)$  where  $E_A$  is the  $A(100)$  torelon energy). Thus the correlation has a constant component in  $t$  (from the torelon contribution) as well as the usual  $\cosh[m_g(t - T/2)]$  term from the glueball contribution. Unfortunately there is no way to estimate reliably the relative size of these two contributions since  $\langle A | P | A \rangle$  is unknown. Assuming that it is of the same order of magnitude as  $\langle g | P | g \rangle$  suggests that correlations for which  $\lambda_g^t < \lambda_A^T$  are suspect. For our studies at  $\beta = 2.9$ , this corresponds to  $t > 3$  for the  $E^+$  state. We see no sign of any such constant term in our results, however.

For the  $A_1^+$  glueball state, one must subtract the vacuum component in creating a suitable path  $P$ . Taking this into account the correlation has corrections from torelon propagation given by

$$\langle P_0 P_t \rangle = \langle g | P | g \rangle^2 (\lambda_g^t + \lambda_g^{T-t}) / (1 + 3\lambda_A^T) + 3(\langle 0 | P | 0 \rangle - \langle A | P | A \rangle)^2 \lambda_A^T$$

where  $|0\rangle$  is the vacuum state. Again a constant in  $t$  is present. The size of this constant is determined by the extent of the cancellation in the last term. Empirically we find a strong cancellation since  $\langle g | P | g \rangle / \langle 0 | P | 0 \rangle \approx 0.1$  while no constant term is apparent in the measured results.

Analysis of torelon contaminations to other glueball states can be made similarly. There are also torelon contaminations to the extraction of torelon energies themselves of course. For the ground-state  $A(100)$  torelon, no constant terms arise since other torelons ( $B(110)$  etc) are heavier. For the extraction of the  $B(110)$  and  $A(110)$  torelon energies, however, there is *a priori* an important constant contribution from  $A(100)$  torelons (e.g. an  $x$ -directed torelon from 0 to  $t$  and a  $y$ -directed torelon from  $t$  to 0 round the back where the appropriate path  $P$  has  $xy$  electric flux). Our results of table 9 perhaps show some signs of this contribution.

## References

- [1] Michael C 1990 *Nucl. Phys. (Proc. Suppl.)* B **17** 59
- [2] Decker K and de Forcrand Ph 1990 *Nucl. Phys. (Proc. Suppl.)* B **17** 567

- [3] Teper M 1987 *Phys. Lett.* **183B** 345
- [4] Michael C and Teper M 1987 *Phys. Lett.* **199B** 95; 1988 *Nucl. Phys. B* **305** 453
- [5] Albanese M *et al* 1987 *Phys. Lett.* **192B** 163
- [6] Michael C and Perantonis S J 1990 *Nucl. Phys.* **347B** 854
- [7] Michael C, Huntley A and Perantonis S J 1989 *Nucl. Phys. B* **326** 544
- [8] Parisi G *et al* 1983 *Phys. Lett.* **128B** 418
- [9] Alvarez O 1981 *Phys. Rev. D* **24** 440
- [10] Arvis J F 1983 *Phys. Lett.* **127B** 106
- [11] Ding H Q, Baillie C F and Fox G C 1990 *Phys. Rev. D* **41** 2912  
Ding H Q *Cal. Tech. preprints* C3P919, C3P959
- [12] de Forcrand P *et al* 1985 *Phys. Lett.* **160B** 137
- [13] Koller J and van Baal P 1988 *Nucl. Phys. B* **302** 1
- [14] Michael C 1987 *J Phys. G: Nucl. Phys.* **13** 1001